Volume 9
Number 5
7 March 2025
Pages 1133–1390

Sustainable Energy & Fuels

Interdisciplinary research for the development of sustainable energy technologies

rsc.li/sustainable-energy

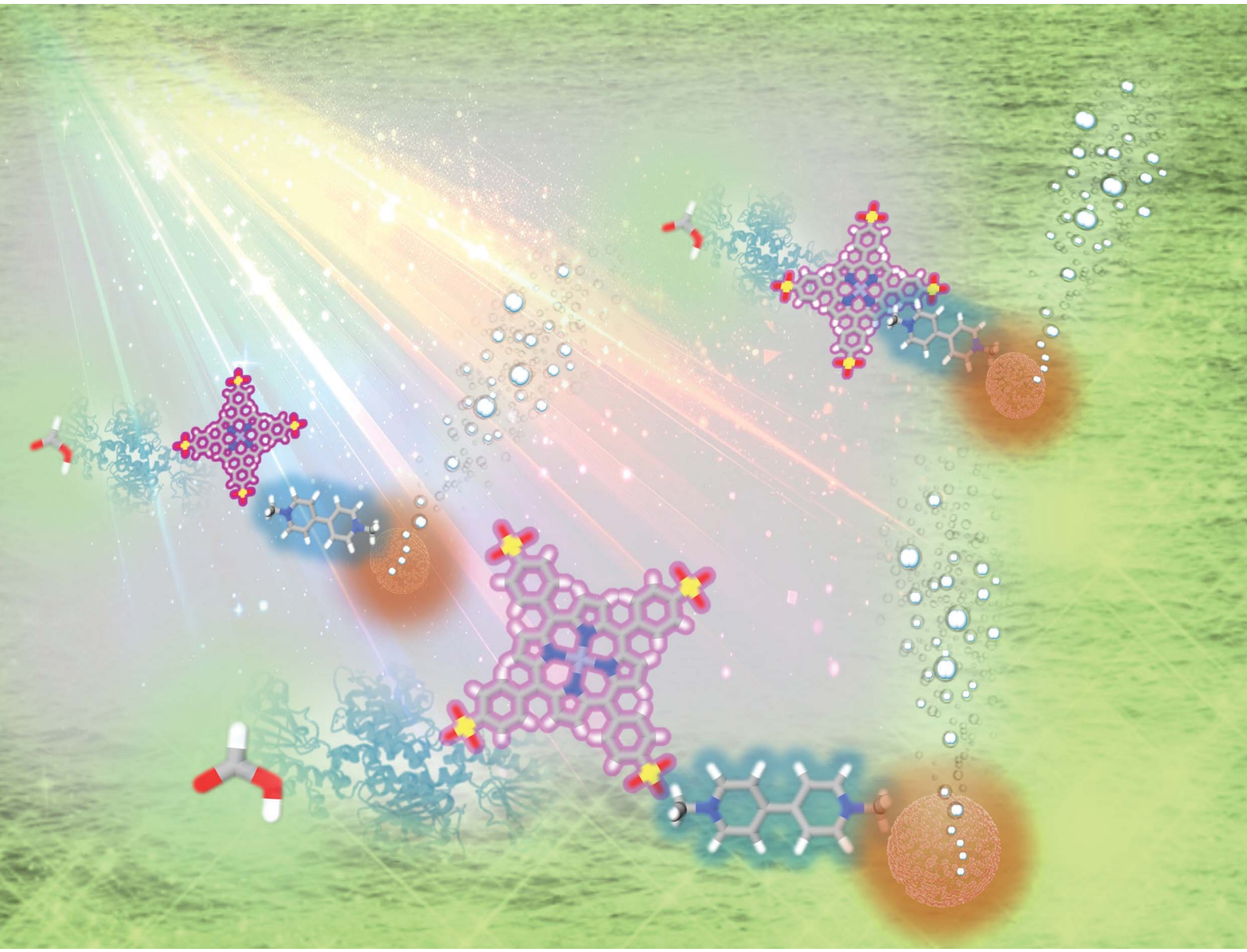

ISSN 2398-4902

ROYAL SOCIETY OF CHEMISTRY

COMMUNICATION

Shintaro Yoshikawa and Yutaka Amao

Visible-light responsive hydrogen production from formate with a photoredox system using enzymes and colloidal platinum nanoparticles

Sustainable Energy & Fuels

ROYAL SOCIETY OF CHEMISTRY

COMMUNICATION

View Article Online
View Journal | View Issue

Cite this: *Sustainable Energy Fuels*, 2025, **9**, 1160

Received 6th September 2024
Accepted 7th January 2025

DOI: 10.1039/d4se01245c

rsc.li/sustainable-energy

Visible-light responsive hydrogen production from formate with a photoredox system using enzymes and colloidal platinum nanoparticles†

Shintaro Yoshikawa[a] and Yutaka Amao *[ab]

Formic acid and formate are among the most promising candidates for hydrogen energy carriers that can be produced from carbon dioxide. As previously reported, H_2 production based on catalytic formate decomposition involves two major issues: the use of strong acidic formate with relatively low pH and reaction control after catalyst addition. To address these two issues, visible-light controlled H_2 production from formate with the combination system of a bio-catalytic process with formate dehydrogenase from *Candida boidinii* (CbFDH) and a photoredox reaction of water-soluble zinc porphyrin, methylviologen and colloidal platinum nanoparticles dispersed in polyvinylpyrrolidone (Pt-PVP) was developed. By using this system, the yield for formate to H_2 was estimated to be *ca.* 92% after 25 h irradiation.

Formic acid has a hydrogen capacity of 4.3 wt% (53 g L^{-1}) and is of growing interest as a promising hydrogen carrier.[1,2] The carbon dioxide–formic acid cycle is expected to be a simple and environmentally friendly hydrogen storage and release process.[3] To decompose formate into H_2 and CO_2 selectively, various heterogeneous or homogeneous catalysts containing metals have been studied. For examples of metal-based heterogeneous catalysts, palladium nanoparticles immobilised on inorganic supports and alloy materials containing palladium have been widely studied as heterogeneous catalysts for H_2 production based on formate decomposition.[4–9] Homogeneous molecular catalysts based on coordination complexes containing metal ions such as Ir^{3+}, Rh^{3+}, and Ru^{3+} have also been widely investigated as highly active catalysts for H_2 production based on formate decomposition.[10–16] In contrast, we devoted to colloidal platinum nanoparticles dispersed by a water-soluble polymer with the H_2 production catalytic function as a homogeneous catalyst. It was found that colloidal platinum nanoparticles dispersed in polyvinylpyrrolidone (Pt-PVP) catalyse H_2 production based on formate decomposition.[17–21] Fig. 1 shows the pH dependence of H_2 production based on formate decomposition with Pt-PVP[18] and the mechanism for H_2 production.[21] The H_2 production shown in Fig. 1 is the amount after 3 h incubation.

As shown in Fig. 1, H_2 production reaches a maximum around the pK_a (3.75) of formic acid. In other words, in formate decomposition with Pt-PVP, H_2 production decreases with increasing pH. When formic acid is used safely as a hydrogen carrier, it is more preferable to use it in a formate solution near neutral pH. In addition, the availability of neutral to weakly basic pH solutions allows the simultaneous production of CO_2 based on formate decomposition to be fixed in solution as bicarbonate. For example, a study on the practical application of a cycling system for H_2 production from potassium formate and hydrogenation of potassium bicarbonate has been reported.[22] The volumetric energy density of formate is lower compared to formic acid. However, the safety and toxicological aspects of formate, as well as its sustainability, make it ideal as a hydrogen storage system. Formate is non-corrosive, non-

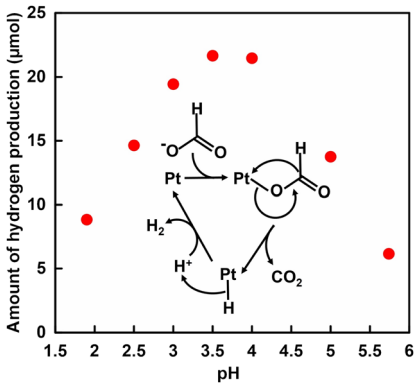

Fig. 1 The pH dependence of H_2 production based on formate decomposition with Pt-PVP. Inset: possible mechanism for H_2 production from formate with Pt-PVP.

[a]*Graduate School of Science, Osaka Metropolitan University, 3-3-138 Sugimoto, Sumiyoshi-ku, Osaka 558-8585, Japan. E-mail: amao@omu.ac.jp*

[b]*Research Centre of Artificial Photosynthesis (ReCAP), Osaka Metropolitan University, 3-3-138 Sugimoto, Sumiyoshi-ku, Osaka 558-8585, Japan*

† Electronic supplementary information (ESI) available. See DOI: https://doi.org/10.1039/d4se01245c

irritant, non-toxic, and easy to handle as a hydrogen energy carrier. Another problem with the thermal H_2 production system based on formate decomposition is that H_2 production cannot be controlled once the reaction is initiated by the addition of a catalyst. Therefore, we focused on formate dehydrogenase catalysed formate oxidation in the presence of NAD^+ under conditions in the neutral pH range.[23,24] In particular, FDH from *Candida boidinii* (CbFDH) is commercially available and widely used as a catalyst for the reduction of CO_2.[25–27] On the other hand, one approach for controlling hydrogen production is the use of a photoredox system consisting of an electron-donating molecule, visible photosensitising molecule, electron mediator molecule and catalysts. Visible-light driven H_2 production with the system of triethanolamine (TEOA) as an electron donor, water-soluble zinc porphyrin, zinc meso-tetra(4-sulfonatophenyl)porphyrin tetrasodium salt ($ZnTPPS^{4-}$) as a visible photosensitizer, methylviologen (MV^{2+}) as an electron mediator and colloidal platinum nanoparticles or hydrogenase as a catalyst has been reported.[28–30] NADH, as well as TEOA, has been reported to act as an electron donor in this system.[28] Thus, by using redox coupling between NAD^+ and NADH, visible light-driven H_2 production from formate can be achieved as shown in Fig. 2.

In this study, visible-light controlled H_2 production from formate with the combination system of a biocatalytic process with CbFDH and a photoredox reaction of $ZnTPPS^{4-}$, MV^{2+} and Pt-PVP was investigated.

First, visible-light driven H_2 production with the system of sodium formate, CbFDH, NAD^+, $ZnTPPS^{4-}$, MV^{2+} and Pt-PVP in phosphate buffer (pH 7.0) was investigated. Details of the materials used and all experimental procedures are described in the ESI (Fig. S1(a) and (b)†). The amount of formate was estimated by ion chromatography with an ion exclusion column. Fig. S2† shows the chromatogram of sodium formate (0–100 mM) in 500 mM-HEPES buffer (pH 7.0). The inset of Fig. S2† shows the relationship between the sodium formate concentration and the detection peak area. The amount of H_2 and CO_2 production was determined using a gas chromatograph (GC-2014, SHIMADZU Corporation) with a thermal conductivity detector (TCD). The calibration curve for the determination of the amount of H_2 and CO_2 by gas chromatograph is shown in Fig. S3, S4, eqn S2 and S3,† respectively. Fig. 3 shows the time dependence of the amount of formate, H_2 and CO_2 in the sample solution with irradiation. As shown in Fig. 3, H_2 and CO_2 were produced with irradiation time. On the other hand, formate was decreased with reaction time. After 5 h irradiation, 33.9 μmol of H_2 was produced and the yield for formate to hydrogen was estimated to be *ca.* 68%. In addition, formate

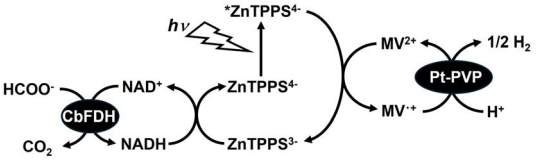

Fig. 2 Visible-light driven H_2 production from formate with the system of CbFDH, NAD^+, $ZnTPPS^{4-}$, MV^{2+} and Pt-PVP.

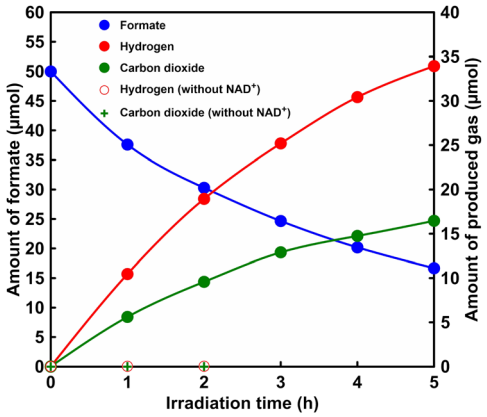

Fig. 3 Time dependence of H_2 and CO_2 production, and formate consumption with the system of sodium formate (50 μmol) CbFDH (0.95 U; *ca.* 24 nmol), NAD^+ (25 μmol), $ZnTPPS^{4-}$ (50 nmol), MV^{2+} (0.25 μmol) and Pt-PVP (0.25 μmol) in phosphate buffer solution (pH 7.0) during visible-light irradiation. H_2 (○) and CO_2 (+) production without NAD^+ conditions during visible-light irradiation.

consumption was estimated to be *ca.* 33.3 μmol. The amount of formate consumed was equivalently related to the amount of H_2 produced.

In contrast, 16.5 μmol of CO_2 was produced after 5 h reaction time. CO_2 was detected at about half the amount of H_2 produced. It is important to note that the detected amount of carbon dioxide is present in the gas phase of the reaction vessel. The mole fractions of CO_2, bicarbonate and carbonate in the solution at pH 7.0 are estimated to be 11.3, 88.5 and 0.2% respectively. After 25 h irradiation, 9.0% hydrochloric acid solution was added to the sample solution and stirred under dark conditions for 1 h to adjust the pH to 1.5. After this procedure, the gas phase was analysed by gas chromatography. 45 and 37 μmol of H_2 and CO_2 were detected in the gas phase, respectively. The results support that by lowering the pH of the sample solution to the acidic side, bicarbonate was converted to CO_2 and transferred to the gas phase. Thus, this suggests that the remaining CO_2 dissolves as bicarbonate in solution. After 25 h irradiation, moreover, 45.8 μmol of H_2 was produced and the yield for formate to H_2 was estimated to be *ca.* 92%. After 25 h of visible-light irradiation, thus, the initial formate was completely converted to H_2. Next let us discuss the tolerance of this system. The change in the UV-visible absorption spectra of the reaction solution during irradiation was measured. Fig. S5† shows the time dependence of difference spectra in the sample solution from before to after light irradiation (inset: UV-vis absorption spectrum of $ZnTPPS^{4-}$). As shown in Fig. S5,† the absorption bands of $ZnTPPS^{4-}$ (420, 555 and 595 nm) decreased with light irradiation. The reduced concentration of $ZnTPPS^{4-}$ was calculated to be approximately 4.8 μM (24 nmol), and it is estimated that approximately half of the $ZnTPPS^{4-}$ was decomposed after 5 h irradiation. Next, let us discuss the tolerance of CbFDH in this system. After 25 h irradiation, the formate was almost consumed, thus, 50 μmol of sodium formate was added to evaluate the remaining activity of CbFDH. After 5 h of re-addition of sodium formate, approximately 8

μmol was consumed during irradiation as shown in Fig. S6.† Thus, CbFDH-catalysed formate oxidation proceeds, but the catalytic activity is predicted to decrease over time. Let us compare this system with H_2 production by photolysis of water using a visible light-responsive photocatalyst such as poly(-heptazine imides),[31] CoO_x and Rh/Cr_2O_3 on poly(triazine imide).[32] It is difficult to make a simple comparison between H_2 production using water as an electron source and based on formate decomposition because the purposes are different; however, the wavelength range of visible light that can be used by these photocatalysts is often at the long wavelength end of 500 nm. The advantage of this system is that by using $ZnTPPS^{4-}$ as a sensitizer, it is expected that H_2 production can be achieved using visible light more than 500 nm. Fig. S7(a)† shows the time dependence of H_2 and CO_2 production with irradiation through the optical filter Y52 (the characteristic of the optical filter Y52 is shown in Fig. S7(b)†), which transmits wavelengths above 520 nm. As shown in Fig. S7(a),† H_2 and CO_2 were produced with irradiation time. After 5 h irradiation, 17.0 and 10.1 μmol of H_2 and CO_2 were produced. Although the amount of hydrogen produced was less than that without the optical filter, H_2 production was achieved even with irradiation with visible light more than 520 nm. Next, it was confirmed that H_2 and CO_2 were produced from formate in the system shown in Fig. 2. In the presence of NADH, CO_2 production proceeds based on formate oxidation catalysed by CbFDH. In addition, it has been reported that visible light-driven H_2 production proceeds using a system composed of NADH, $ZnTPPS^{4-}$, MV^{2+} and Pt-PVP.[28] It has also been reported that H_2 production based on formate decomposition catalysed by Pt-PVP does not proceed under pH 7 conditions.[18] Because the CbFDH-catalysed formate oxidation and visible-light-driven H_2 production are linked by the NAD^+/NADH redox cycle, removing NAD^+ from the system should result in neither CO_2 nor H_2 being produced. As shown in Fig. 3, when the system consisting of sodium formate, CbFDH, $ZnTPPS^{4-}$, MV^{2+} and Pt-PVP, in other words, excluding NAD^+ was irradiated with visible light, no H_2 and CO_2 were produced. In other words, the CbFDH-catalysed formate oxidation and the visible light-driven H_2 production *via* the NAD^+/NADH redox cycle as shown in Fig. 2 were accomplished.

Next, pH dependence of the visible-light driven H_2 production with the system of sodium formate, CbFDH, NAD^+, $ZnTPPS^{4-}$, MV^{2+} and Pt-PVP in phosphate buffer was investigated. Fig. 4 shows the time dependence of H_2 (a) and CO_2 (b) in the sample solution of sodium formate, CbFDH, NAD^+, $ZnTPPS^{4-}$, MV^{2+} and Pt-PVP with the irradiation under pH conditions of 6.0, 7.0 and 8.0. As shown in Fig. 4, 2.06, 33.9 and 22.4 μmol of H_2 were produced under pH conditions of 6.0, 7.0 and 8.0 after 5 h irradiation, respectively. In contrast, 2.50, 16.8 and 3.98 μmol of CO_2 were produced under pH conditions of 6.0, 7.0 and 8.0 after 5 h irradiation, respectively. The production of H_2 and CO_2 was found to be dependent on the pH of the sample solution. In terms of H_2 production, the highest hydrogen production occurred under pH 7.0 conditions of the sample solution, while H_2 production decreased under pH 8.0 and 6.0 conditions. The lowest H_2 production was observed under pH 6 conditions with a high concentration of H^+

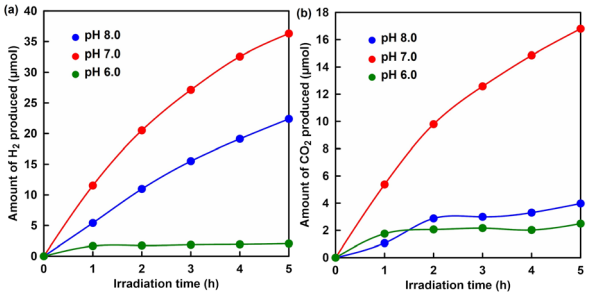

Fig. 4 Time dependence of H_2 (a) and CO_2 production (b), and formate consumption with the system of sodium formate (50 μmol) CbFDH (0.95 U; *ca.* 24 nmol), NAD^+ (25 μmol), $ZnTPPS^{4-}$ (50 nmol), MV^{2+} (0.25 μmol) and Pt-PVP (0.25 μmol) in various pH phosphate buffer solutions during visible-light irradiation.

compared to other conditions. Also, it was found that CO_2 production was lower than that under other pH conditions. Here, the reduction of NAD^+ to NADH based on the oxidation of formate catalysed by CbFDH proceeds irrespective of visible light irradiation or non-irradiation. Fig. S9† shows the relationship between the initial concentration of NAD^+ and the reaction rate for NADH production due to formate oxidation with CbFDH under various pH conditions.

As shown in Fig. S9,† the rate for formate oxidation was significantly decreased at pH 6 and the optimum pH for CbFDH-catalysed formate oxidation was around 7, so under pH 6 conditions, NADH production was decreased due to the reduced catalytic activity of CbFDH for formate oxidation. In the visible light-driven H_2 production system comprising $ZnTPPS^{4-}$, MV^{2+} and Pt-PVP, NADH acts as an electron donor, suggesting that under pH 6 conditions, H_2 production was reduced due to lower NADH production following CbFDH-catalysed formate oxidation. Under pH 8 conditions, on the other hand, the amount of H_2 produced was about 0.66 times lower than that under pH 7 conditions. This is predicted to be due to a decrease in the amount of H^+ with increasing pH. On the other hand, a significant decrease in CO_2 production was observed compared to hydrogen production under pH 8.0 conditions. It has been reported that the catalytic activity of CbFDH for the oxidation of formate is not significantly reduced under pH 8 conditions. It is predicted that most of the CO_2 produced is dissolved as bicarbonate in a buffer solution at pH 8. The amount of CO_2 production shown in Fig. 4(b) is the result of quantifying the gas phase of the reaction vessel by gas chromatography. This means that under pH 8 conditions, it was suggested that more than 80% of the CO_2 produced was fixed as bicarbonate in the buffer solution. These results show that the system can efficiently produce H_2 under pH 7 conditions, and that neutral formate can be used as a raw material instead of strong acidic formic acid.

Finally, the visible light control of H_2 production using the system of sodium formate, CbFDH, NAD^+, $ZnTPPS^{4-}$, MV^{2+} and Pt-PVP in phosphate buffer (pH 7) was investigated. Fig. 5 shows the time dependence of the amount of formate, H_2 and CO_2 in the sample solution during the light-on/off cycle. As shown in Fig. 5, formate was consumed with reaction time irrespective of

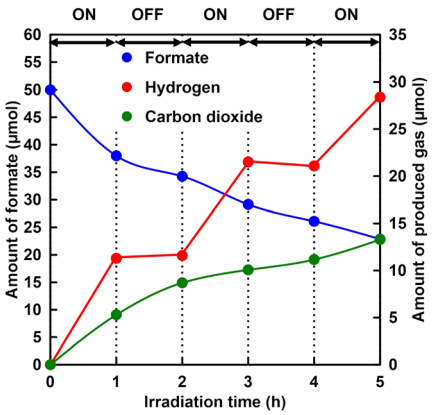

Fig. 5 Time dependence of H_2 and CO_2 production, and formate consumption with the system of sodium formate (50 μmol), CbFDH (0.95 U; *ca.* 24 nmol), NAD^+ (25 μmol), $ZnTPPS^{4-}$ (50 nmol), MV^{2+} (0.25 μmol) and Pt-PVP (0.25 μmol) in phosphate buffer solution (pH 7.0) under visible-light irradiation on/off conditions.

irradiation or non-irradiation. Also, CO_2 was produced with reaction time irrespective of irradiation or non-irradiation. In contrast, H_2 was produced in response to irradiation and stopped completely under non-irradiation conditions. Thus, NADH produced during CbFDH-catalysed formate oxidation accumulates under dark conditions, but direct electron transfer from the produced NADH to Pt-PVP does not proceed and H_2 production is suppressed. In addition, H_2 production based on formate decomposition catalysed by Pt-PVP is also suppressed under neutral pH conditions. Finally, let us discuss the catalytic activity of Pt-PVP in this reaction system. As colloidal Pt-PVP consists of platinum atoms on the surface and in the bulk, the catalytically active sites are likely to be platinum atoms on the surface of Pt-PVP. According to previous reports, the amount of platinum atoms on the surface is calculated to be 0.11 μmol.[33,34] Thus, the turnover number (TONs) of Pt-PVP for H_2 production from formate solution in this system was determined to be 255. Furthermore, NAD^+/NADH recycling was also achieved, as the amount of H_2 production was observed above the initial amount of NAD^+.

In conclusion, visible-light controlled H_2 production from formate with the combination system of a biocatalytic process with CbFDH and a photoredox reaction of $ZnTPPS^{4-}$, MV^{2+} and Pt-PVP was developed and formate was completely converted to H_2 after 25 h irradiation under pH 7 conditions. On the other hand, it was also shown that approximately half of the CO_2 produced during formate decomposition is fixed as bicarbonate in a buffer solution at pH 7.

Data availability

The authors confirm that the data supporting the findings of this manuscript are available within the article and its ESI.†

Conflicts of interest

There are no conflicts to declare.

Acknowledgements

This work was partially supported by a grant-in-aid for specially promoted Research (23H05404), and Scientific Research (B) (22H01872), (22H01871).

Notes and references

1 J. Yang, A. Sudik, C. Wolverton and D. J. Siegel, *Chem. Soc. Rev.*, 2010, **39**, 656.
2 A. K. Singh, S. Singh and A. Kumar, *Catal. Sci. Technol.*, 2016, **6**, 12.
3 H. Zhong, M. Iguchi, M. Chatterjee, Y. Himeda, Q. Xu and H. Kawanami, *Adv. Sustainable Syst.*, 2018, **2**, 1700161.
4 D. A. Bulushev, L. J. Jia, S. Beloshapkin and J. R. H. Ross, *Chem. Commun.*, 2012, **48**, 4184.
5 D. A. Bulushev, S. Beloshapkin, P. E. Plyusnin, Y. V. Shubin, V. I. Bukhtiyarov, S. V. Korenev and J. R. H. Ross, *J. Catal.*, 2013, **299**, 171.
6 Y. Zhao, L. Deng, S. Y. Tang, D. M. Lai, B. Liao, Y. Fu and O. X. Guo, *Energy Fuels*, 2011, **25**, 3693.
7 B. J. O'Neill, E. I. Gürbüz and J. A. Dumesic, *J. Catal.*, 2012, **290**, 193.
8 O. Metin, X. L. Sun and S. H. Sun, *Nanoscale*, 2013, **5**, 910.
9 K. Mori, M. Dojo and H. Yamashita, *ACS Catal.*, 2013, **3**, 1114.
10 Y. Himeda, S. Miyazawa and T. Hirose, *ChemSusChem*, 2011, **4**, 487.
11 Y. Himeda, *Green Chem.*, 2009, **11**, 2018.
12 Y. Himeda, N. Onozawa-Komatsuzaki, H. Sugihara and K. Kasuga, *Organometallics*, 2007, **26**, 702.
13 Y. Himeda, N. Onozawa-Komatsuzaki, H. Sugihara, H. Arakawa and K. Kasuga, *Organometallics*, 2004, **23**, 1480.
14 J. F. Hull, Y. Himeda, W. H. Wang, B. Hashiguchi, R. Periana, D. J. Szalda, J. T. Muckerman and E. Fujita, *Nature Chem.*, 2012, **4**, 383.
15 S. Fukuzumi, T. Kobayashi and T. Suenobu, *ChemSusChem*, 2008, **1**, 827.
16 A. Boddien, B. Loges, H. Junge and M. Beller, *ChemSusChem*, 2008, **1**, 751.
17 Y. Minami, Y. Muroga, T. Yoshida and Y. Amao, *Chem. Lett.*, 2019, **48**, 775.
18 Y. Minami and Y. Amao, *Sustainable Energy Fuels*, 2020, **4**, 3458.
19 Y. Minami, Y. Muroga and Y. Amao, *New J. Chem.*, 2020, **44**, 14334.
20 Y. Minami and Y. Amao, *New J. Chem.*, 2021, **45**, 11461.
21 Y. Minami and Y. Amao, *J. Jpn. Petrol. Inst.*, 2021, **64**, 203.
22 R. Sang, C. A. M. Stein, T. Schareina, Y. Hu, A. Léval, J. Massa, V. Turan, P. Sponholz, D. Wei, R. Jackstell, H. Junge and M. Beller, *Nature Commun.*, 2024, **15**, 7268.
23 W. Hummel and M. R. Kula, *Eur. J. Biochem.*, 1989, **184**, 1.
24 J. G. Ferry, *FEMS Microbiol. Rev.*, 1990, **7**, 377.
25 J. H. Kim, D. H. Nam and C. B. Park, *Curr. Opin. Biotechnol.*, 2014, **28**, 1.
26 S. K. Kuk, R. K. Singh, D. H. Nam, R. Singh, J. K. Lee and C. B. Park, *Angew. Chem., Int. Ed.*, 2017, **56**, 3827.

27 H. Wu, C. Tian, X. Song, C. Liu, D. Yang and Z. Jiang, *Green Chem.*, 2013, **15**, 1773.
28 Y. Amao, *ChemCatChem*, 2011, **3**, 458.
29 Y. Amao and I. Okura, *J. Mol. Catal. A:Chem.*, 1996, **105**, 125.
30 N. Kaji, S. Aono and I. Okura, *J. Mol. Catal.*, 1986, **36**, 201–203.
31 Q. Wang, S. Li, D. Zheng, S. Wang, Y. Hou and G. Zhang, *ACS Appl. Energy Mater.*, 2024, **7**, 6090.
32 M. Liu, G. Zhang, X. Liang, Z. Pan, D. Zheng, S. Wang, Z. Yu, Yi. Hou and X. Wang, *Angew. Chem., Int. Ed.*, 2023, **62**, e202304694.
33 H. Kotani, R. Hanazaki, K. Ohkubo, Y. Yamada and S. Fukuzumi, *Chem. Eur. J.*, 2011, **17**, 2777.
34 Y. Matsubara, Y. Muroga, M. Kuwata and Y. Amao, *Sustainable Energy Fuels*, 2022, **6**, 3717.

